

# Near-Optimal Midcourse Guidance for Air-to-Air Missiles

P. K. A. Menon\*

*Georgia Institute of Technology, Atlanta, Georgia 30332*  
and

M. M. Briggs†

*Integrated Systems, Inc., Santa Clara, California 95054*

Singular perturbation theory is used to derive a near-optimal mid-course guidance law incorporating a linear combination of flight time and terminal specific energy as the performance index. State variables in the slow time-scale model consist of down range, cross range, specific energy, and heading angle. A near-optimal approach using feedback linearization is developed to account for altitude and flight-path-angle dynamics neglected in the slow time-scale solution. Implementation logic and simulation results for an engagement scenario are given.

## Introduction

THE problem of near-optimal missile guidance during the midcourse phase has been of significant interest in recent literature.<sup>1,2</sup> This paper outlines an approach to this problem using a reduced-order model and boundary-layer correction method different from those considered in Refs. 1 and 2. The guidance law development has its roots in singular perturbation theory.<sup>3</sup> Singular perturbation theory aids in splitting the optimal guidance problem into a series of low-order subproblems that may be sequentially solved and later combined to obtain an approximate solution to the full-order problem. The key idea involved here is the separation of dynamics based on the notion of slow and fast state variables. The slowest time-scale solution is called the "outer solution," and the correction terms accounting for higher-order dynamics are called "boundary-layer corrections." This terminology has its roots in the theory of viscous fluids, where such a structure was first exploited.<sup>3</sup>

This approach is attractive for the midcourse guidance problem primarily because the optimal control formulation with complete missile point-mass model produces a 12th-order two-point boundary-value problem,<sup>4</sup> which is impossible to solve numerically on any present-day onboard computers in real time. These problems require a considerable amount of computing resources and are prone to numerical instabilities of various kinds. For this reason, techniques based on singular perturbation theory provide a viable real-time approach for the midcourse guidance problem.

A survey of existing literature reveals that a variety of guidance laws have been derived using singular perturbation theory.<sup>1-3,5-10</sup> The chief differences between these are in time-scale separation and the boundary-layer correction method. A survey of various time-scale separation possibilities have been examined in Ref. 11. Near-optimality of some of these guidance laws have been previously established.<sup>6,12</sup> In the present

paper, four state variables will be treated in the outer solution, and the boundary-layer correction will address the altitude and flight-path-angle dynamics. Even though the time-scale separation employed in this paper is similar to that in Ref. 8, the present analysis exploits certain available features of the slow time-scale problem to reduce onboard storage and execution time. It is important to also note that, unlike Ref. 8, the performance index in the present formulation incorporates a linear combination of flight time and terminal specific energy. Inclusion of terminal energy is motivated by the fact that a high terminal energy is essential for minimizing the miss distance in the end game. A near-optimal boundary-layer correction approach based on feedback linearization<sup>13</sup> will be employed in the present work. This approach assumes that, in the boundary layer, the energy-heading dynamics can be approximated by a quadratic form in altitude, altitude rate, and vertical acceleration. This approximation appears to be valid in airframes with a quadratic drag polar. A boundary-layer correction using the method of individual time scales<sup>14</sup> for the present guidance problem has been discussed in Ref. 15.

Additionally, as in Refs. 1 and 2, the missile guidance problem will be treated here as a one-side optimization problem, although it should be modeled as a differential game.<sup>16</sup> This treatment necessarily assumes that the target motions can be predicted in each guidance interval. Thus, a predicted intercept point is computed in each guidance interval, which is then used as the terminal conditions for the missile. Consequently, a new optimization problem is solved from the current conditions to the predicted terminal conditions in every guidance step. Whenever the missile is within the onboard seeker lock-on range, a terminal guidance scheme such as proportional navigation<sup>4</sup> or a more advanced guidance law<sup>17</sup> is used to accomplish target intercept.

## Vehicle Modeling

The point-mass equations of motion for a missile flying over a flat, nonrotating Earth with a quiescent atmosphere is given by

$$\dot{E} = \frac{V(T - D)}{mg} \quad (1)$$

$$\dot{\phi} = \frac{gn_h}{V \cos \gamma} \quad (2)$$

Received Dec. 3, 1987; revision received Dec. 19, 1988. Copyright © 1989 American Institute of Aeronautics and Astronautics, Inc. All rights reserved.

\*Associate Professor, School of Aerospace Engineering. Member AIAA.

†Manager, Missile Systems Division. Associate Fellow AIAA.

$$\dot{x} = V \cos \gamma \cos \phi \quad (3)$$

$$\dot{y} = V \cos \gamma \sin \phi \quad (4)$$

$$\dot{h} = V \sin \gamma \quad (5)$$

$$\dot{\epsilon} \gamma = \frac{g}{V} (n_v - \cos \gamma) \quad (6)$$

where  $E$  is the specific energy,  $\gamma$  the flight-path angle,  $\phi$  the heading angle,  $T$  the vehicle thrust,  $D$  the vehicle drag,  $g$  the acceleration due to gravity, and  $m$  the vehicle mass. Position of the missile in an Earth-fixed, inertial frame is given by the down range  $x$ , cross range  $y$  and altitude  $h$ . The control variables in this model are horizontal and vertical components of the load factor,  $n_h$  and  $n_v$ , respectively. Use of this form for the control variables instead of the more familiar bank angle and load factor has been shown to reduce algebraic complexity.<sup>7</sup> Transformation from one form to another is straightforward. The parameter  $\epsilon$  appended on the right-hand side of Eqs. (5) and (6) serves to denote that these variables evolve on a faster time scale than others. Thus, with  $\epsilon = 0$  one obtains the slow time-scale problem whereas setting this parameter to unity yields the complete system.

In Eqs. (1-6), the variable  $V$  should be interpreted as a shorthand notation for

$$V = \sqrt{2g(E - h)} \quad (7)$$

In the present analysis, the aerodynamic drag is calculated using the following expressions:

$$D = D_0 + D_i(n_v^2 + n_h^2) \quad (8)$$

$$D_0 = C_{D_0} Q_s \quad (9)$$

$$D_i = m^2 g^2 R, \quad R = K/Q_s, \quad Q = \rho V^2/2 \quad (10)$$

where  $C_{D_0}$  is the zero-lift drag coefficient and  $K$  the induced drag coefficient, both given as functions of Mach number;  $\rho$  the atmosphere density;  $s$  the reference area; and  $Q$  the dynamic pressure.

### Midcourse Guidance Law

The optimal guidance problem analyzed in this paper may be defined as

$$\min_{n_v, n_h} \left[ -\zeta E(t_f) + (1 - \zeta) \int_0^{t_f} dt \right] \quad (11)$$

subject to the differential constraints [Eqs. (1-6)] with initial conditions specified for all the state variables. The final time  $t_f$  is open. The missile is required to reach the predicted target intercept point  $x_f, y_f$  while minimizing the performance index [Eq. (11)] and satisfying initial conditions. The weighting factor  $\zeta$  enables the tradeoff between flight time and terminal energy. This factor is constrained as

$$0 \leq \zeta \leq 1 \quad (12)$$

The terminal energy maximization term included in the performance index explicitly recognizes the fact that a high terminal energy is essential for minimizing the miss distance in the homing guidance phase. Additionally, the guidance solution should satisfy the following inequality constraints:

$$Q_{\min} \leq Q \quad (13)$$

$$\sqrt{n_v^2 + n_h^2} \leq |n_{\max}| \quad (14)$$

The minimum dynamic pressure constraint (13) is imposed here to insure adequate aerodynamic controllability of the missile. Missile structural integrity requirements dictate the load factor limit in Eq. (14). It is interesting to note that, unlike aircraft, the missile stall angle-of-attack limit is seldom reached during the midcourse guidance phase. Additionally, it has been observed that the commanded flight altitude seldom violates the terrain limit.

If the optimal control problem is formulated based on the foregoing, a 12th-order two-point boundary-value problem will result. Admittedly, it is possible to generate off-line numerical solutions. The interest in singular perturbations theory stems from the fact that these calculations can often be very time-consuming and are prone to various numerical instabilities. Using singular perturbation theory, the guidance problem may be broken up into subproblems based on the speed of state variable evolution. The slowest time-scale problem is solved first, followed by a sequential solution of the faster subproblems. This process yields a relatively robust, near-optimal nonlinear feedback law for the midcourse guidance problem.

Guidance law derivation using singular perturbation theory will be discussed in the ensuing. As indicated elsewhere in this paper, four state variables are treated in the outer solution:  $x$ ,  $y$ ,  $E$ , and  $\phi$ . Altitude and flight-path-angle dynamics are included as boundary-layer corrections.

Two techniques for generating boundary-layer corrections for the altitude and flight-path-angle dynamics were originally developed.<sup>15</sup> First of these is the treatment of altitude and flight-path angle in separate time scales as in Ref. 14, whereas the second approach is based on feedback linearization.<sup>13</sup> In the first case, the guidance problem will have three time scales: a slow time scale handling down range, cross range, specific energy, and heading angle dynamics; a fast time scale accounting for altitude dynamics; and a very fast time scale providing for flight-path-angle dynamics.

In boundary-layer correction method using feedback linearization, the time-scale separation employed is of the form 1) slow time scale:  $x$ ,  $y$ ,  $E$ , and  $\phi$ ; and 2) fast time scale:  $h$  and  $\gamma$ . This paper will discuss the second boundary-layer correction approach together with the outer solution.

### Outer Solution

The outer problem can be obtained by assuming that the fast variables are in equilibrium in the slow time scale. This is equivalent to setting  $\epsilon = 0$  in the vehicle model given by Eqs. (1-6). This process yields the differential equations (1-4) along with the algebraic constraints

$$n_{v1} = 1, \quad \gamma_1 = 0 \quad (15)$$

where the subscript 1 denotes the values of state and control variables in a slow time scale.

In the outer solution, the aerodynamic drag is computed using  $n_{v1} = 1$  as required by expression (15). Control variables in this time scale are the horizontal component of load factor  $n_{h1}$  and the altitude  $h_1$ . Variational Hamiltonian<sup>4</sup> in this time scale can be formulated as

$$h_1 = \lambda_{x1} V_1 \cos \phi_1 + \lambda_{y1} V_1 \sin \phi_1 + \lambda_{E1} \left\{ \frac{V_1(T - D_1)}{mg} \right\} + \lambda_{\phi1} \frac{g n_h}{V_1} + (1 - \zeta) \quad (16)$$

The terminal transversality condition yields the final value of the specific energy costate as

$$\lambda_{E1}(t_f) = -\zeta \quad (17)$$

An appropriate set of boundary conditions will now be defined for cross range and heading angle to permit a direct reduced-order system solution.

Following Ref. 7, it will be assumed that the terminal value of heading angle  $\phi_1(t_f)$  is free. It will subsequently be seen that, using this formulation, it is still possible to reach the desired final heading asymptotically. Next, it is assumed that the final value of  $y$  is free. With this, one has

$$\lambda_{y_1} = 0, \quad \lambda_{x_1} = \text{const} \quad (18)$$

$$\dot{\lambda}_{\phi_1} = \lambda_{x_1} \dot{y} \quad (19)$$

Equation (19) may be integrated to yield

$$\lambda_{\phi_1} = -\lambda_{x_1}(\psi_f - y) \quad (20)$$

In Eq. (20),  $y_f$  is the cross range at the final time, and  $y$  is the current value of cross range. The natural boundary condition  $\lambda_{\phi_1}(t_f) = 0$  has been employed in obtaining Eq. (20). It is clear that the terminal condition on the heading angle costate will be met if the missile cross range reaches the target cross range  $y_f$  at the final time.

Additionally, invoking the transversality condition for the free final time problem,  $H_1(t_f) = 0$ , it is possible to compute the down-range costate  $\lambda_{x_1}$  as

$$\lambda_{x_1} = \left[ \frac{\zeta \{T(t_f) - D_1(t_f)\}}{m_f g} - \frac{(1 - \zeta)}{V_1(t_f)} \right] \frac{1}{\cos \phi_1(t_f)} \quad (21)$$

where  $m_f$  is the missile mass at the final time. The final value of thrust  $T(t_f)$  is included in Eq. (21) in order to account for a final thrust impulse, sometimes used to augment missile maneuverability in the end game. It is important to note that although  $V_1(t_f)$  can be obtained as the airspeed at the dash point for aircraft,<sup>3</sup> this quantity has to be estimated using various approximations<sup>1,2</sup> for missiles without air-breathing propulsion.

Next, the optimal horizontal component of the load factor may be calculated from the optimality condition

$$\partial H_1 / \partial n_{h_1} = 0$$

This yields

$$n_{h_1} = \frac{\lambda_{\phi_1}}{\lambda_{E_1}} \left( \frac{mg^2}{2V_1^2 D_i} \right) = \frac{-\lambda_{x_1}}{\lambda_{E_1}} \left( \frac{mg^2}{2V_1^2 D_i} \right) (\psi_f - y) \quad (22)$$

whenever  $n_{h_1}$  is less than the specified load factor limit. Otherwise,  $n_{h_1}$  should be chosen to satisfy the inequality constraint

$$\sqrt{1 + n_{h_1}^2} \leq |n_{\max}| \quad (23)$$

Expression (22) is a nonlinear feedback law that produces a horizontal component of load factor in the presence of a cross-range error. From Eq. (22), since  $\lambda_{\phi_1}(t_f) = 0$ , it is clear that  $n_{h_1} = 0$  at the final time. This suggests that the final value of drag  $D_1(t_f)$  required for the calculation of  $\lambda_{x_1}$  in Eq. (21) may be computed as the symmetric flight drag with  $n_{v_1} = 1$ .

At this point, an approximation<sup>1,2</sup> will be introduced for computing the specific energy costate  $\lambda_{E_1}$ . Since the missile thrust and mass depend explicitly on time, the variational Hamiltonian (16) is not autonomous. Following Refs. 1 and 2, the thrust and mass are next replaced by their average values. This permits one to invoke a constant of motion; i.e.,  $H_1(t) = 0$ . This averaging is based on the remaining time of flight. Previous research<sup>1,2</sup> has shown that this is a reasonable assumption. Thus, one has

$$H_1(t) = a + b\lambda_{E_1} + c/\lambda_{E_1} = 0 \quad (24)$$

where

$$a = \lambda_{x_1} V_1 \cos \phi_1 + (1 - \zeta) \quad (25)$$

$$b = \frac{V_1(T_{\text{av}} - D_0 - D_i)}{m_{\text{av}} g} \quad (26)$$

$$c = \lambda_{\phi_1}^2 \left( \frac{mg^3}{2V_1^3 D_i} \right) \left( \frac{2m_{\text{av}} - m}{2m_{\text{av}}} \right) \quad (27)$$

where  $m_{\text{av}}$  and  $T_{\text{av}}$  are the average thrust and mass of the missile, respectively. If  $\lambda_{E_1}$  is not zero, Eq. (24) may be multiplied by this quantity to obtain a quadratic in  $\lambda_{E_1}$ . This quadratic can then be solved for obtaining the specific energy costate in the slow time scale. The roots of this quadratic are given by

$$\lambda_{E_1} = \frac{-a \pm \sqrt{a^2 - 4bc}}{2b} \quad (28)$$

The root that produces the appropriate sign for the optimal horizontal component of the load factor should be used in subsequent calculations. Whenever the missile is in symmetric flight,  $c = 0$  and the roots are given by

$$\lambda_{E_1} = -\frac{[\lambda_{x_1} V_1 + (1 - \zeta)]m_{\text{av}} g}{V_1(T_{\text{av}} - D_0 - D_i)}, \quad 0 \quad (29)$$

It is interesting to note here that, if one substitutes for the costate  $\lambda_{x_1}$  from Eq. (21) with  $\phi_1 = \zeta = 0$  and replaces  $T_{\text{av}}$  and  $m_{\text{av}}$  by their actual values, expression (29) will reduce to that obtained for optimal symmetric aircraft trajectories.<sup>18</sup>

The final step in the computation of the reduced-order solution is that of determining the optimal altitude  $h_1$ , the second control variable in this time scale. This calculation employs the condition,  $\partial H_1 / \partial h_1 = 0$ . Differentiating the variational Hamiltonian with respect to altitude and equating to zero, one has

$$0 = -\lambda_{x_1} g \cos \phi_1 - \lambda_{E_1} \left[ \frac{T - D_0 - D_i}{m} + \frac{V_1^2}{mg} \left\{ \frac{\partial D_0}{\partial h_1} + \frac{\partial D_i}{\partial h_1} \right\} \right] + n_{h_1} \left[ \frac{\lambda_{E_1} D_i n_{h_1}}{m} - \frac{\lambda_{E_1} V_1^2 n_{h_1}}{mg} \frac{\partial D_i}{\partial h_1} + \frac{\lambda_{\phi_1} g^2}{V_1^2} \right] \quad (30)$$

The preceding expression implicitly determines the value of optimal altitude. If desired, one may substitute the values of  $\lambda_{\phi_1}$ ,  $\lambda_{x_1}$ , and  $\lambda_{E_1}$  from Eqs. (20), (21), and (29) to obtain an expression that depends only on the system states. In the interest of conserving space, this step will not be carried out here. It may be observed that the optimal altitude calculation constitutes the most difficult part of the present optimal guidance law calculation. Details of this calculation will be given in a subsequent discussion on implementation aspects.

As mentioned elsewhere in this paper, the guidance solution has to satisfy the minimum dynamic pressure constraint. Since altitude is a control variable in the slow time scale, this constraint can be imposed as an altitude limit; i.e.,

$$Q_{\min} - \rho g(E - h_{\max}) \leq 0 \quad (31)$$

At each energy level, expression (31) may be solved as an equality to obtain the maximum permissible missile altitude. Because of the dependence of  $\rho$  on altitude, expression (31) implicitly determines the constrained altitude. If the optimal altitude calculated using expression (30) exceeds that given by expression (31), then the latter value should be used in subsequent calculations.

This completes the outer solution calculations. To summarize the foregoing material, the outer solution produces optimal values of altitude  $h$  and horizontal component of the load factor  $n_h$  using the current values of  $y$ ,  $\phi$ ,  $E$ ,  $T$ ,  $m$ ,  $D_0$ ,  $D_i$ ; and the estimated values of  $\phi(t_f)$ ,  $V(t_f)$ ,  $y_f$ , and  $t_f$ .

### Boundary-Layer Correction

The outer solution obtained in the foregoing handles all but the altitude and flight-path-angle dynamics. This solution can be implemented onboard a missile only if these results are corrected for neglected altitude and flight-path-angle dynamics. In the terminology of singular perturbation theory, these are referred to as the boundary-layer corrections. Only zeroth-order boundary-layer corrections<sup>19</sup> will be discussed in this paper. Because of the highly nonlinear nature of the boundary-layer system arising in atmospheric flight mechanics problems, various approximations have been suggested in the literature.<sup>6,7,10,13,14,19</sup> Two of these, the method of individual time scales<sup>14</sup> and the method of feedback linearization,<sup>13</sup> have been used to explore missile guidance law development.<sup>15</sup> The second method will be discussed in the present paper.

### Boundary-Layer Correction with Feedback Linearization

This boundary-layer correction technique is based on the premise that the chief objective of boundary-layer correction is to generate a stable control law that will permit the missile to follow the outer solution closely. Thus, the implicit assumption here is that the outer variables have the most significant impact on the missile performance, whereas the boundary-layer variables contribute a relatively minor performance improvement. Note that this assumption is consistent with the slow-fast decomposition of the dynamics. If this point of view is adopted, the feedback linearization approach<sup>13</sup> can be used to generate an elegant boundary-layer correction methodology. Effectively, this approach assumes that, in the boundary layer, right-hand sides of the energy-heading equations can be approximated by a quadratic form in altitude, altitude rate, and vertical acceleration. This is a reasonable assumption in airframes with approximately quadratic drag polar. The resulting boundary-layer correction is in the form of an asymptotically stable nonlinear feedback law, useful for generating near-optimal initial and terminal boundary-layer corrections.

An important advantage of this approach is that the altitude and flight-path-angle dynamics need not be separated, since the feedback linearization approach can handle high-order dynamics without difficulty. Another interesting aspect is that one may select the speed of evolution and damping for the boundary-layer variables to ensure adequate time-scale separation while satisfying the specified control constraints. Additionally, this approach can accommodate improved slow time-scale solutions obtained using alternate slow-fast variables as in Refs. 20 and 21. In contrast with the linearized approach for boundary-layer correction<sup>3,10,19</sup> for atmospheric flight mechanics problems, the feedback linearization approach is valid even for large deviations between the values of fast variables in the outer and inner layers. However, note that the present approach for boundary-layer correction is feasible only if a feedback linearizing transformation can be found for the boundary-layer system.

The zeroth-order boundary-layer problem<sup>19</sup> is formally obtained by introducing a time-stretching transformation  $\tau = t/\epsilon$  in system (1-6) and considering the limit as  $\epsilon$  tends to zero. Under this condition, the system [Eqs. (1-6)] becomes

$$E' = 0, \quad \phi' = 0 \quad (32)$$

$$h_2' = \sqrt{2g(E_1 - h_2)} \sin \gamma_2 \quad (33)$$

$$\gamma_2' = \frac{g}{\sqrt{2g(E_1 - h_2)}} (n_{v_2} - \cos \gamma_2) \quad (34)$$

where

$$' \equiv \frac{d}{d\tau}$$

and where the subscript 2 denotes the variables in a fast time scale. Expression (32) suggests that the specific energy and the heading angle remain frozen in the boundary layer. The boundary-layer dynamics are given by expressions (33) and (34). The integrand of the performance index in the boundary layer is given by the last three terms in Eq. (16), viz., the slow time-scale Hamiltonian evaluated in the fast time scale.<sup>3</sup> Because of the time-stretching transformation employed in the boundary layer, integration limits for this performance index are from zero to infinity. Note that the differential equations for  $x$  and  $y$  have been dropped from consideration in the fast time scale because these are cyclic variables. Next, as in the singular perturbation theory for feedback systems,<sup>22</sup> consider the difference between the fast time-scale variables in the outer and inner problems as

$$\Delta h = h_2 - h_1, \quad \Delta \gamma = \gamma_2 - \gamma_1, \quad \Delta n_v = n_{v_2} - n_{v_1} \quad (35)$$

it is important to note that  $\Delta h$ ,  $\Delta \gamma$ , and  $\Delta n_v$  are not restricted to small quantities in the ensuing analysis. The boundary-layer equations of motion in these variables can be written as

$$\Delta h' = \sqrt{2g(E_1 - h_1 - \Delta h)} \sin(\Delta \gamma + \gamma_1) \quad (36)$$

$$\Delta \gamma' = \frac{g}{\sqrt{2g(E_1 - h_1 - \Delta h)}} [(\Delta n_v + n_{v_1}) - \cos(\Delta \gamma + \gamma_1)] \quad (37)$$

where the subscript 1 denotes the state and control variables from the outer solution. Note that, if the outer solution discussed in an earlier section of this paper is used,  $\gamma_1 = 0$  and  $n_{v_1} = 1$ . On the other hand, if one employs improved outer solutions obtained through a better choice of state variables such as those proposed in Refs. 21 and 22,  $\gamma_1$  may not be zero. Thus, in the interests of preserving generality, these substitutions will not be made explicitly in the ensuing development.

The objective of boundary-layer correction is to optimally drive  $\Delta h$ ,  $\Delta \gamma$  to zero. Note that the boundary-layer system is highly nonlinear. If the performance index in the boundary-layer problem is approximated by a quadratic form in  $\Delta h$ ,  $\Delta h'$ ,  $\Delta h''$ , asymptotically stable nonlinear feedback laws can be synthesized for this system using prelinearizing transformation theory.<sup>13,22</sup> Such an approximation appears to be valid for flight vehicles with a quadratic drag polar.

Differentiating expression (36) with respect to  $\tau$  and substituting for  $\Delta h'$  and  $\Delta \gamma'$ , one has

$$\Delta H' = \Delta h'' = g \Delta n_v \cos(\Delta \gamma + \gamma_1) + g [n_{v_1} \cos(\Delta \gamma + \gamma_1) - 1] \quad (38)$$

$$\Delta h' = \Delta H \quad (39)$$

In Eqs. (38) and (39) the variable  $\Delta \gamma + \gamma_1$  should be interpreted as

$$\Delta \gamma + \gamma_1 = \sin^{-1} \left[ \frac{\Delta H}{\sqrt{2g(E_1 - h_1 - \Delta h)}} \right] \quad (40)$$

Next the system [Eqs. (38) and (39)] can be put in feedback linearized form by replacing the right-hand side of expression (38) by a pseudo-control variable  $U$ . This yields

$$\Delta H' = U \quad (41)$$

$$\Delta h' = \Delta H \quad (42)$$

A feedback control law may now be synthesized for the linear time-invariant system (41) and (42) to minimize the boundary-layer performance index approximated by a quadratic form in  $\Delta h$ ,  $\Delta H$ , and  $U$ . This controller can be obtained using linear quadratic regulator theory,<sup>4</sup> via the algebraic Riccati equation. The state and control weighting matrices in the quadratic criterion can be determined by fitting a

quadratic in  $\Delta h$ ,  $\Delta H$ ,  $U$  to the variational Hamiltonian in the slow time scale, evaluated using the boundary-layer variables. Alternately, if the question of optimality with respect to the original criterion is set aside in the boundary layer, these matrices can be chosen to maintain adequate time-scale separation while restricting the control variable to remain within the given bounds. In either case, the resulting control law will be of the form

$$U = G_1 \Delta H + G_2 \Delta h \quad (43)$$

Feedback gains  $G_1$  and  $G_2$  are computed using the algebraic Riccati equation. The pseudo-control variable calculated in Eq. (43) can be transformed to real controls as

$$\Delta n_v = \frac{G_1 \Delta H + G_2 \Delta h - g [n_{v1} \cos(\Delta \gamma + \gamma_1) - 1]}{g \cos(\Delta \gamma + \gamma_1)} \quad (44)$$

The total value of the vertical component of the load factor in the boundary layer can then be obtained as

$$n_{v2} = \Delta n_v + n_{v1} \quad (45)$$

This completes the altitude and flight-path-angle boundary-layer calculations. As indicated in the foregoing, performance requirements other than the optimality with respect to the quadratic criterion can be imposed on the boundary-layer system. This may be in the form of a natural frequency  $\omega$  and a damping ratio  $\xi$ . Equivalently, the rise time and percentage overshoot may be specified. If this were done, the feedback gains  $G_1$  and  $G_2$  may be expressed in terms of the natural frequency and damping ratio as

$$G_1 = -2\xi\omega, \quad G_2 = -\omega^2 \quad (46)$$

The latter approach has the advantage of being able to control the speed of boundary-layer evolution, an important consideration in ensuring the validity of applying singular perturbation theory to the present guidance problem.

An important consequence of the boundary-layer correction method described here is that the evolution of the boundary-layer variables in the stretched time scale can be written down in closed form. Thus,

$$\Delta H(\tau) = e^{-c_0 \tau} [c_1 \sin(\omega_d \tau - \chi) + c_2 \sin \omega_d \tau] \quad (47)$$

$$\Delta h(\tau) = e^{-c_0 \tau} [c_4 \sin(\omega_d \tau - \chi) + c_3 \sin \omega_d \tau] \quad (48)$$

where

$$c_0 = \xi\omega, \quad c_1 = \frac{\Delta H(0)}{\sqrt{1-\xi^2}}, \quad c_2 = -\Delta h(0)\omega \quad (49)$$

$$c_3 = \frac{\Delta H(0) + 2\xi\omega\Delta h(0)}{\omega\sqrt{1-\xi^2}}, \quad c_4 = \frac{\Delta h(0)}{\sqrt{1-\xi^2}} \quad (50)$$

$$\omega_d = \omega\sqrt{1-\xi^2}, \quad \chi = \left[ \frac{\sqrt{1-\xi^2}}{\xi} \right] \quad (51)$$

These expressions are useful for computing the range covered during the altitude/flight-path-angle transition from the given boundary conditions to the outer solution values. An estimate of these quantities is important to ensure satisfactory guidance law performance for arbitrary launch ranges. For instance, before attempting to climb to the optimal altitude calculated by the outer solution, the guidance scheme must ensure that the range to the target is greater than the sum of range to climb to the optimal altitude and the range required for descent to the target altitude.<sup>23</sup>

Assuming that the vehicle is in symmetric flight, the down-range equation is given by

$$x' = \sqrt{2g(E_1 - h_1)} (1 + \delta)^{1/2} \quad (52)$$

where

$$\delta = -\frac{\Delta h}{E_1 - h_1} - \frac{\Delta H^2}{2g(E_1 - h_1)} \quad (53)$$

Expression (52) has used the fact that  $V_2 = \sqrt{[2g(E_1 - h_1 - \Delta h)]}$  and that the flight-path-angle  $\gamma_2$  is calculated using expression (40). Expanding the right-hand side of Eq. (52) in a binomial series and retaining the first two terms of the expression, and integrating, one has

$$x(\tau) = \sqrt{2g(E_1 - h_1)}\tau - \frac{\sqrt{2g}}{2\sqrt{E_1 - h_1}}x_1 - \frac{1}{2\sqrt{2g(E_1 - h_1)}}x_2 \quad (54)$$

where

$$x_1 = \frac{e^{-c_0 \tau}}{c_0^2 + \omega_d^2} \left[ (c_0 c_4 \cos \chi + c_3 c_0 - c_4 \omega_d \sin \chi) \sin \omega_d \tau - [(c_4 \cos \chi + c_3) \omega_d + c_4 c_0 \sin \chi] \cos \omega_d \tau \right] \quad (55)$$

$$x_2 = -\frac{e^{-c_0 \tau}}{4c_0} \left[ (c_1 \cos \chi + c_2)^2 + (c_1 \sin \chi)^2 \right] - \frac{e^{-2c_0 \tau} \cos 2\omega_d \tau}{4c_0^2 + 4\omega_d^2} \left[ c_0(c_1 \cos \chi + c_2)^2 - c_0(c_1 \sin \chi)^2 + (c_1 \cos \chi + c_2)2\omega_d c_1 \sin \chi \right] - \frac{e^{-2c_0 \tau} \sin 2\omega_d \tau}{4c_0^2 + 4\omega_d^2} \left[ -(c_1 \cos \chi + c_2)^2 \omega_d + (c_1 \sin \chi)^2 \omega_d + (c_1 \cos \chi + c_2)2c_0 c_1 \sin \chi \right] \quad (56)$$

For calculating range for climb or descent, the time to reach 95 or 99% of the commanded altitude from the starting conditions is first calculated using expressions (47) and (48). Let this time be  $\tau_s$ . Substituting  $\tau = \tau_s$  in expression (54) will yield the range covered for climb or descent. In general, there would be an initial climb segment from the launch altitude to the optimal altitude and a terminal descent to the target altitude. The range covered in both these maneuvers can be calculated using Eq. (54).

Once these quantities are available, a logic may be set up for adjusting the optimal altitude based on estimated range-to-go. This is essential so that at relatively shorter ranges the missile does not climb so high that it overshoots the target. Some additional details on this calculation will be given while the implementation aspects are discussed.

### Guidance Law Evaluation

The guidance law obtained in the foregoing section was implemented on an existing beyond-visual-range missile simulation.<sup>1,2</sup> This simulation uses a six-degree-of-freedom model of a tactical air-to-air missile including sensor/actuator dynamics and error models. In its present form, the simulation employs a linear interpolation scheme for aerodynamic and atmospheric data. The equations of motion are integrated using a fourth-order Runge-Kutta scheme. This simulation also includes a target model. The target model is capable of maneuvering in a pseudointelligent manner,<sup>1,2</sup> or can maneuver using an evasion logic based on differential game theory.<sup>17</sup>

Implementation details of the guidance law will be outlined in the following. As mentioned elsewhere, the guidance law uses both on-line and off-line calculations. Each of these will be separately discussed in the following.

### Off-Line Calculations

The results of off-line calculations are stored in a tabular form onboard and are used for on-line guidance law computation. The first step here is the selection of the weighting factor  $\zeta$ , between final energy and time. A specific choice of this factor may be based on simulations of various operational engagement scenarios. Second, the guidance law calculations require the zero-lift drag and induced drag components at each energy and altitude levels. Since the aerodynamic coefficients are known a priori, these may be precomputed and stored in the form of two-dimensional tables. Typically the following quantities are stored:

$$D_0(E, h), \quad R(E, h), \quad \frac{\partial D_0}{\partial h}(E, h), \quad \frac{\partial R}{\partial h}(E, h) \quad (57)$$

$R$  has been defined in Eq. (10). Elsewhere in this paper, it has been shown that minimum dynamic pressure constraint can be imposed as a maximum altitude constraint in the outer solution. Thus, within the range of energies of interest, a one-dimensional table of the form  $h_{\max}(E)$  can also be constructed and stored.

### On-Line Calculations

In each guidance interval, on-line calculations required in the guidance law consist of the following:

- 1) Estimate the predicted values of time of flight  $t_f$ , the intercept point  $x_f, y_f$ , terminal airspeed  $V_1(t_f)$ , and the terminal value of the heading angle  $\phi_1(t_f)$  using any reasonable method.<sup>1,2</sup>
- 2) Compute drag at the final time.
- 3) Compute the range costate  $\lambda_x$  using Eq. (21).
- 4) Calculate the current value of the heading angle costate  $\lambda_{\phi_1}$  using Eq. (20).
- 5) Using the estimated time-to-go, calculate the average thrust and mass.

These computations are followed by an iterative calculation for optimal altitude. The sequence of computations includes the following:

- 1) Guess an initial value of optimal altitude  $h_1$ . As in Ref. 23, these calculations may be accelerated by using the optimal altitude from the previous guidance step as the initial guess.
- 2) Using the current value of specific energy and  $h_1$ , calculate the airspeed  $V_1$ . The energy costate  $\lambda_{E_1}$  is then computed using Eq. (28).
- 3) Using  $V_1, \lambda_{E_1}, \lambda_{\phi_1}$ , the induced drag term  $D_i$ , and the current value of mass, calculate the horizontal component of load factor  $n_h$ . This computation will employ expression (22).
- 4) Calculate the quantity on the right-hand side of Eq. (30), the optimality condition for the outer solution altitude.
- 5) If this quantity is sufficiently close to zero, continue. Otherwise, change the guessed altitude and go back to step 2.

A one-dimensional minimization scheme can perform this iterative calculation. Numerical results given in this paper

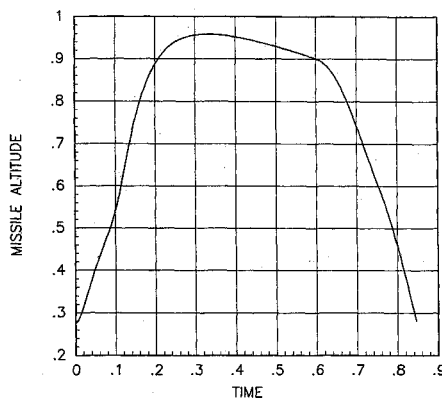


Fig. 1 Normalized altitude vs normalized time.

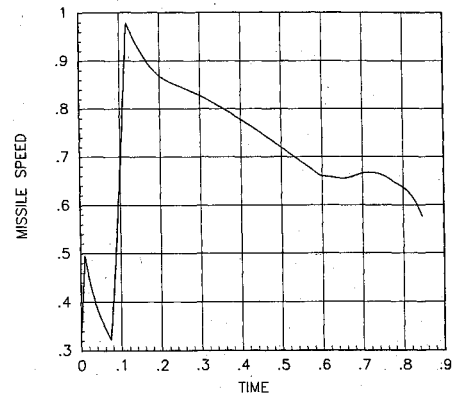


Fig. 2 Normalized airspeed vs normalized time.

were generated using the method of bisections. Three or four iterations are often adequate to meet the desired accuracy requirements. This completes the calculation of the outer solution. In the following, computations involved in boundary-layer corrections will be sketched.

Though two boundary-layer correction approaches were developed for the present research,<sup>15</sup> only the technique based on feedback linearization has been implemented. The logic in the following, however, is equally valid for both approaches. In the present work, the outer solution requires the missile to climb to the optimal altitude and fly at the optimal altitude until it reaches the vicinity of the target. At that point, a descent to the target altitude is initiated. Since altitude is a control variable in the slow timescale, the outer solution assumes that the initial climb and terminal descent take place instantaneously. The climb and descent flight segments require finite amounts of range, however. Consequently, one must insure that sufficient range is available for performing the climb-cruise-descend flight paths. If the intercept range is not adequate to carry out these maneuvers, the missile has to essentially use a cruise altitude lower than the optimal altitude. This computation requires the following iteration:

- 1) From the current altitude, altitude rate, and the optimal altitude calculated from the outer solution, determine the range covered for climb using Eq. (54). Let this be  $x_c$ . Using the estimated terminal speed and target altitude, estimate the terminal optimal altitude. Using the terminal optimal altitude and the target altitude, compute the range required for descent once again by using Eq. (54). Let this quantity be  $x_d$ .
- 2) If  $x_c + x_d$  is less than the estimated range-to-go, compute the boundary-layer correction using the procedure discussed. Otherwise, update the optimal altitude, and go to step 1.

In the present work, the method of bisections is also employed for these calculations. With this, the guidance law calculations are complete. Outputs of the guidance algorithm are the vertical and horizontal components of load factor  $n_v, n_h$ , which form the autopilot inputs.

Though several trajectory runs have been made at the time of this writing, only one of them will be discussed in this paper. The engagement scenario chosen to illustrate the guidance law performance features a nonmaneuvering target in symmetric flight near the missile outer launch boundary. Subsequent to launch from an aircraft, the missile flies level for a fixed amount of time to insure adequate separation from the launch aircraft. After this time period, it climbs to the optimal altitude computed by the outer solution. The missile continues to track the commanded altitude until it reaches the target vicinity. At a calculated range-to-go, the descent to target altitude is initiated. The seeker lock-on occurs subsequently, and from that point on, the missile employs a homing guidance scheme.

All of the three phases discussed earlier can be observed in a plot of normalized altitude vs normalized time given in Fig. 1. From this figure, the continuous decrease in optimal cruise altitude due to energy depletion can clearly be observed. The

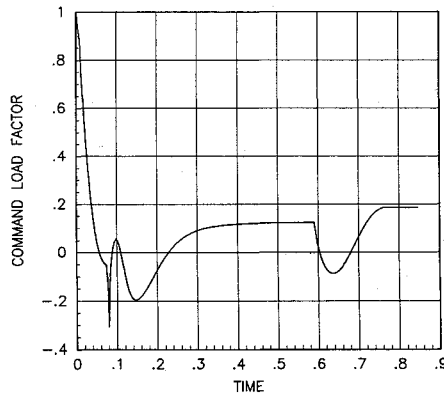


Fig. 3 Normalized load factor vs normalized time.

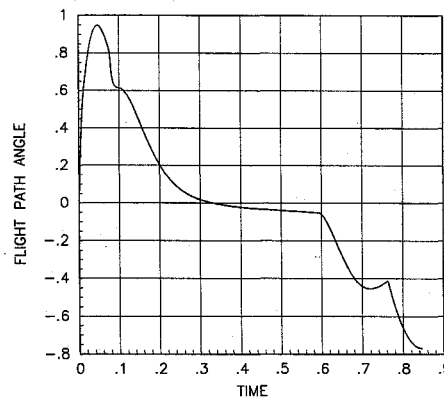


Fig. 4 Normalized flight-path angle vs normalized time.

different climb rates seen in Fig. 1 arise due to the two-pulse motor-propulsion system employed in the missile. Normalized airspeed corresponding to this trajectory is given in Fig. 2. A decreased deceleration during missile cruise at the optimal altitude may be observed in this figure. Load factor history for this trajectory is shown in Fig. 3. Negative excursions in the load factor history are caused by the ignition and burnout energy transients arising from the second pulse. The load factor is close to the outer solution value throughout the optimal altitude cruise region. A corner appearing in the load factor history at descent initiation arises from the range matching calculations discussed earlier. The flight-path-angle history in Fig. 4 shows that it remained close to zero throughout the cruise region with initial and terminal transients.

Additional simulation runs are being made currently for comparing the present guidance law with that reported in Ref. 1. Additionally, the effect of the parameter  $\zeta$  on the guidance solution is also being evaluated.

### Conclusions

A midcourse guidance law for air-to-air missiles was derived in this paper using singular perturbation theory. This guidance law is based on a four-state outer solution featuring down range, cross range, specific energy, and heading angle as the slow state variables. This solution yields optimal values of altitude and the horizontal component of the load factor using the current values of cross range, heading angle, specific energy, thrust, drag, mass, and estimated final values of airspeed, heading angle, cross range, and flight time.

The boundary-layer correction handles the altitude and flight-path-angle dynamics. A near-optimal feedback linearization approach was proposed for altitude/flight-path-angle boundary layer. This approach was shown to yield additional quantities useful for guidance law implementation. Details on guidance law implementation and simulation results were given.

### Acknowledgments

This research was supported by the Air Force Rocket Propulsion Laboratory, Edwards Air Force Base, California, under Contract F04611-85-C-0082, with Lt. Mark Beyer serving as the Technical Monitor. The authors thank Daniel J. Lesieutre of Nielson Engineering and Research and Gano B. Chatterji of Integrated Systems, Inc., for their help in generating the numerical results given in this paper.

### References

- <sup>1</sup>Cheng, V. H. L., and Gupta, N. K., "Advanced Midcourse Guidance for Air-to-Air Missiles," *Journal of Guidance, Control, and Dynamics*, Vol. 8, No. 2, 1986, pp. 103-107.
- <sup>2</sup>Cheng, V. H. L., Menon, P. K. A., Gupta, N. K., and Briggs, M. M., "Reduced-Order Pulse-Motor Ignition Control Logic," *Journal of Guidance, Control, and Dynamics*, Vol. 10, No. 4, 1987, pp. 343-350.
- <sup>3</sup>Kelley, H. J., "Aircraft Maneuver Optimization by Reduced-Order Approximation," *Control and Dynamic Systems*, edited by C. T. Leondes, Academic, New York, 1973, pp. 131-178.
- <sup>4</sup>Bryson, A. E., and Ho, Y. C., *Applied Optimal Control*, Hemisphere, Washington, DC, 1975.
- <sup>5</sup>Calise, A. J., "Singular Perturbation Techniques for On-line Flight-Path Control," *Journal of Guidance and Control*, Vol. 4, No. 4, 1981, pp. 398-405.
- <sup>6</sup>Weston, A. R., Cliff, E. M., and Kelley, H. J., "Onboard Near-Optimal Climb-Dash Energy Management," *Journal of Guidance, Control, and Dynamics*, Vol. 8, No. 3, 1985, pp. 320-324.
- <sup>7</sup>Visser, H. G., Kelley, H. J., and Cliff, E. M., "Energy Management of Three-Dimensional Minimum-Time Intercept," AIAA Paper 85-1781, Aug. 1985.
- <sup>8</sup>Rajan, N., and Ardema, M. D., "Interception in Three Dimensions: An Energy Formulation," AIAA Paper 83-2121, Aug. 1983.
- <sup>9</sup>Shinar, J., "Validation of Zero-Order Feedback Strategies for Medium Range Air-to-Air Interception in a Horizontal Plane," NASA TM-84237, April 1982.
- <sup>10</sup>Mehra, R. K., Washburn, R. B., Sajan, S., and Carroll, J. V., "A Study of the Application of Singular Perturbation Theory," NASA CR-3167, Aug. 1979.
- <sup>11</sup>Ardema, M. D., and Rajan, N., "Separation of Time Scales in Aircraft Trajectory Optimization," *Journal of Guidance, Control, and Dynamics*, Vol. 8, No. 2, 1985, pp. 275-278.
- <sup>12</sup>Cheng, V. H. L., Menon, P. K. A., and Lin, C. A., "Near-Optimality of a Singular-Perturbation Midcourse Guidance Law and Pulse-Motor Control for Air-to-Air Missiles," AIAA Paper 86-0445, Jan. 1986.
- <sup>13</sup>Menon, P. K. A., and Briggs, M. M., "Near-Optimal Boundary Layer Correction with Prelinearization," AIAA Paper 87-0127, Jan. 1987.
- <sup>14</sup>Calise, A. J., "A New Boundary Layer Matching Procedure for Singularly Perturbed System," *IEEE Transactions on Automatic Control*, Vol. AC-23, No. 3, 1978, pp. 434-438.
- <sup>15</sup>Menon, P. K. A., and Briggs, M. M., "A Midcourse Guidance Law for Air-to-Air Missiles," AIAA Paper 87-2509, Aug. 1987.
- <sup>16</sup>Isaacs, R., *Differential Games*, Kreiger, Huntington, NY, 1965.
- <sup>17</sup>Menon, P. K. A., "Short-Range Nonlinear Feedback Strategies for Aircraft Pursuit-Evasion," *Second International Symposium on Differential Game Applications*, 1986; also *Journal of Guidance, Control, and Dynamics*, Vol. 12, No. 1, 1989, pp. 27-32.
- <sup>18</sup>Schultz, R., and Zagalsky, N. R., "Aircraft Performance Optimization," *Journal of Aircraft*, Vol. 9, No. 2, 1972, pp. 108-114.
- <sup>19</sup>Ardema, M. D., "Solution of the Minimum Time to Climb Problem by Matched Asymptotic Expansions," *AIAA Journal*, Vol. 14, No. 7, 1976, pp. 843-850.
- <sup>20</sup>Kelley, H. J., Cliff, E. M., and Weston, A. R., "Energy State Revisited," AIAA Paper 83-2138, Aug. 1983.
- <sup>21</sup>Ardema, M. D., and Rajan, N., "Slow and Fast State Variables for Three-Dimensional Flight Dynamics," *Journal of Guidance, Control, and Dynamics*, Vol. 8, No. 4, 1985, pp. 532-535.
- <sup>22</sup>Menon, P. K. A., Badgett, M. E., Walker, R. A., and Duke, E. L., "Nonlinear Flight Test Trajectory Controllers for Aircraft," *Journal of Guidance, Control, and Dynamics*, Vol. 10, No. 1, 1987, pp. 67-72.
- <sup>23</sup>Calise, A. J. and Moerder, D. D., "Singular Perturbation Techniques for Real-Time Aircraft Trajectory Optimization and Control," NASA CR-3597, Aug. 1982.